

# Precision calculations for $\gamma\gamma \rightarrow WW \rightarrow 4 \text{ fermions } (+\gamma)$

A. Bredenstein, S. Dittmaier, M. Roth

*Max-Planck-Institut für Physik, D-80805 München, Germany*

The  $\mathcal{O}(\alpha)$  electroweak radiative corrections to  $\gamma\gamma \rightarrow WW \rightarrow 4f$  within the electroweak Standard Model are calculated in double-pole approximation (DPA). Virtual corrections are treated in DPA, and real-photon corrections are based on complete lowest-order matrix elements for  $\gamma\gamma \rightarrow 4f+\gamma$ . The radiative corrections are implemented in a Monte Carlo generator called COFFER $\gamma\gamma$ <sup>1</sup>, which optionally includes anomalous triple and quartic gauge-boson couplings in addition and performs a convolution over realistic spectra of the photon beams. A brief survey of numerical results comprises  $\mathcal{O}(\alpha)$  corrections to integrated cross sections as well as to angular and invariant-mass distributions.

## 1. INTRODUCTION

As an option at a future  $e^+e^-$  linear collider, a photon (or  $\gamma\gamma$ ) collider [1] found considerable interest in recent years. It could provide us with information about new physics phenomena, such as properties of Higgs bosons or of new particles, which is in many respects complementary in the  $e^+e^-$  and  $\gamma\gamma$  modes (see, e.g., Refs. [1, 2] and references therein). Moreover, a  $\gamma\gamma$  collider is a true W-boson-pair factory, owing to the extremely high W-pair cross section, which tends to a constant of about 80 pb in the high-energy limit (in the absence of phase-space cuts), opening the possibility of precision studies in the sector of electroweak gauge bosons. For instance, an analysis of anomalous gauge-boson couplings in  $\gamma\gamma \rightarrow WW \rightarrow 4f$  provides direct information on the  $\gamma WW$  and  $\gamma\gamma WW$  interactions without interference from the Z-boson sector. Either way, whether one is interested in W-boson precision physics or in the search for new phenomena, precise predictions for W-pair production are indispensable for signal and background studies.

As described in Refs. [3, 4] in detail, we have constructed a Monte Carlo generator called COFFER $\gamma\gamma$  for  $\gamma\gamma \rightarrow 4f$  and  $\gamma\gamma \rightarrow 4f\gamma$ , which particularly focusses on precise predictions for W-pair-mediated final states. Anomalous  $\gamma WW$ ,  $\gamma\gamma WW$ , and  $\gamma\gamma ZZ$  gauge-boson couplings as well as a loop-induced  $\gamma\gamma H$  coupling are optionally included in lowest-order predictions for  $\gamma\gamma \rightarrow 4f$ . Moreover, electroweak radiative corrections of  $\mathcal{O}(\alpha)$  are applied to processes  $\gamma\gamma \rightarrow WW \rightarrow 4f$  in the so-called “double-pole approximation” (DPA). In the following we briefly describe the salient features of COFFER $\gamma\gamma$  and show some sample results. More details and results (also for effects of anomalous couplings) can be found in Refs. [3, 4].

## 2. LOWEST-ORDER PREDICTIONS

In Ref. [3] we have constructed a Monte Carlo event generator for lowest-order predictions based on complete matrix elements for  $\gamma\gamma \rightarrow 4f$ <sup>2</sup> and  $\gamma\gamma \rightarrow 4f\gamma$ . The final-state fermions are treated as massless, but all  $4f$  final states are supported. For  $4f$  production all helicity amplitudes (with and without anomalous couplings) are explicitly given as compact expressions in terms of spinor products. Moreover, the introduction of finite gauge-boson decay widths and the issue of gauge invariance are discussed carefully. The possibility to convolute the cross sections with realistic photon beam spectra is offered upon using the parametrization of COMPAZ [6]. The Standard Model predictions were successfully compared to results obtained with the multi-purpose packages WHIZARD [7] and MADGRAPH [8].

<sup>1</sup>The computer code can be obtained from the authors upon request.

<sup>2</sup>Results for cross sections based on the full set of  $\gamma\gamma \rightarrow 4f$  diagrams were also presented in Ref. [5]. However, no convolution over a realistic photon beam spectrum was performed there.

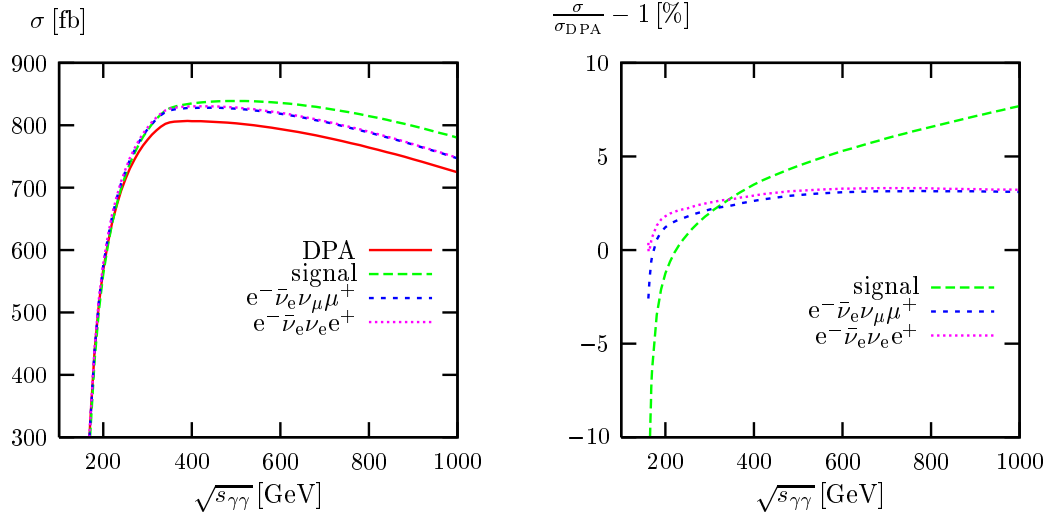


Figure 1: Lowest-order cross sections for  $\gamma\gamma \rightarrow e^-\bar{\nu}_e\nu_\mu\mu^+/e^-\bar{\nu}_e\nu_e e^+$  including all diagrams, only W-pair signal diagrams, and in DPA as a function of the centre-of-mass (CM) energy  $\sqrt{s_{\gamma\gamma}}$  of the monochromatic photon beams (l.h.s.), and the corresponding relative deviations from the DPA (r.h.s.). (Taken from Ref. [3].)

Among the various numerical results shown in Ref. [3], we only highlight the comparison between results that are based on the full set of tree diagrams on the one hand and on the so-called “signal” diagrams that involve two resonant W bosons in  $\gamma\gamma \rightarrow WW \rightarrow 4f$  on the other hand. Of course, the amplitude for this “naive W-pair signal” is not a gauge-invariant quantity. Nevertheless, its investigation is interesting, because such an amplitude is much simpler than the full amplitudes for  $4f$  production and is universal (up to colour factors) for all relevant final states. The DPA for the Born amplitude is obtained from the naive W-pair signal upon deforming the momenta of the four outgoing fermions in such a way that the intermediate W-boson states become on shell, while keeping the W propagators off shell. Since the residues of the W resonances are gauge independent, the Born amplitude in DPA is a gauge-invariant quantity. In Figure 1 the cross sections of the W-pair signal diagrams and the DPA for  $\gamma\gamma \rightarrow WW \rightarrow 4$  leptons are compared with the complete lowest-order cross sections. The plot on the l.h.s. shows the cross sections, the plot on the r.h.s. the relative deviation from the corresponding DPA. We do not include the convolution over the photon spectrum in this analysis so that effects of the approximations are clearly visible. For energies not too close to the W-pair threshold, the DPA agrees with the full lowest-order cross section within 1–3%, which is of the expected order of  $\Gamma_W/M_W$ . Near threshold, i.e. for  $\sqrt{s_{\gamma\gamma}} - 2M_W = \mathcal{O}(\Gamma_W)$ , the reliability of the DPA breaks down, since background diagrams become more and more important and small scales  $\gamma$ , such as  $\sqrt{s_{\gamma\gamma} - 4M_W^2}$ , can increase the naive error estimate from  $\Gamma_W/M_W$  to  $\Gamma_W/\gamma$ . The cross section of the W-pair signal diagrams, however, shows large deviations from the full  $\gamma\gamma \rightarrow 4f$  cross sections for the whole energy range, in particular, at high energies. The results of Figure 1 show that a naive signal definition is a bad concept for  $\gamma\gamma \rightarrow WW \rightarrow 4f$ , since deviations from the full process  $\gamma\gamma \rightarrow 4f$  even reach 5–10% in the TeV range. This is in contrast to the situation at  $e^+e^-$  colliders where the naive W-pair signal (defined in ‘t Hooft–Feynman gauge) was a reasonable approximation (see, e.g., Ref. [9]).

### 3. RADIATIVE CORRECTIONS

#### 3.1. Strategy of the calculation

In Ref. [4] we have extended our lowest-order calculation [3] for  $\gamma\gamma \rightarrow 4f$  by including the electroweak radiative corrections of  $\mathcal{O}(\alpha)$  to the W-pair channels  $\gamma\gamma \rightarrow WW \rightarrow 4f$  in DPA. The DPA extracts those contributions of the  $\mathcal{O}(\alpha)$  corrections that are enhanced by two resonant W-boson propagators, i.e. it represents the leading term in an expansion of the cross section about the two W-propagator poles. Note that tree-level diagrams for  $\gamma\gamma \rightarrow 4f$

with at most one resonant W boson are suppressed w.r.t. the doubly-resonant  $\gamma\gamma \rightarrow WW$  signal by a factor of  $\mathcal{O}(\Gamma_W/M_W) \sim \mathcal{O}(\alpha)$ . Consequently, predictions based on full lowest-order matrix elements for  $\gamma\gamma \rightarrow 4f$  and  $\mathcal{O}(\alpha)$  corrections for  $\gamma\gamma \rightarrow WW \rightarrow 4f$  in DPA should be precise up to terms of  $\mathcal{O}(\alpha/\pi \times \Gamma_W/M_W)$ , since corrections typically involve the factor  $\alpha/\pi$ . Including a quite conservative numerical safety factor, the relative uncertainty should thus be  $\lesssim 0.5\%$  for such predictions, as long as neglected effects are not additionally enhanced. The naive error estimate can, in particular, be spoiled by the occurrence of large scale ratios, which exist, e.g., near production thresholds or at very high energies. The estimate has recently been confirmed for  $e^+e^- \rightarrow WW \rightarrow 4f$  with CM energies  $170 \text{ GeV} \lesssim \sqrt{s} \lesssim 300 \text{ GeV}$  by comparing a full  $\mathcal{O}(\alpha)$  calculation [10] with the corresponding DPA predictions provided by RACOONWW [11].

For energies in the W-pair threshold region ( $\sqrt{s_{\gamma\gamma}} < 170 \text{ GeV}$ ) and below, the DPA is unreliable, because diagrams with at most one resonant W boson become equally important. Therefore, in this region we employ an “improved Born approximation” (IBA) which is based on leading universal corrections but does not involve any resonance expansion. As also confirmed by the full  $\mathcal{O}(\alpha)$  calculation [10] for the related process  $e^+e^- \rightarrow WW \rightarrow 4f$ , such an IBA reproduces the  $\mathcal{O}(\alpha)$ -corrected cross section typically within  $\sim \pm 2\%$ . The convolution of the hard  $\gamma\gamma$  cross section involves both the IBA (in the low-energy tail) and the DPA (for  $\sqrt{s_{\gamma\gamma}} > 170 \text{ GeV}$ ). As shown in Ref. [4], for CM energies (of the electrons before the Compton backscattering)  $\sqrt{s_{ee}} \lesssim 230 \text{ GeV}$  our prediction possesses an uncertainty of  $\sim 2\%$ , because it is mainly based on the IBA, but already for  $\sqrt{s_{ee}} \gtrsim 300 \text{ GeV}$  (500 GeV) the IBA contribution is widely suppressed so that the DPA uncertainty sets the precision of  $\lesssim 0.7\%$  (0.5%) in our calculation.

In detail, we apply the DPA only to the virtual corrections to  $\gamma\gamma \rightarrow WW \rightarrow 4f$ , while we base the real-photon corrections on complete lowest-order matrix elements for  $\gamma\gamma \rightarrow 4f\gamma$ . Apart from the treatment of IR (soft and collinear) singularities, we can use the calculation of the bremsstrahlung processes  $\gamma\gamma \rightarrow 4f\gamma$  for massless fermions described in Ref. [3]. The concept of the DPA was already described in Ref. [12] for the corrections to  $e^+e^- \rightarrow WW \rightarrow 4f$  and later successfully applied to these processes in different versions [11, 13, 14, 15]. We follow the strategy of RACOONWW [11] and adapt it to  $\gamma\gamma$  collisions where necessary. The virtual corrections in DPA can be naturally split into factorizable and non-factorizable contributions. The former comprise the corrections to on-shell W-pair production [16, 17] and the decay [18] of on-shell W bosons. The latter account for soft-photon exchange between the production and decay subprocesses; the known results for the non-factorizable corrections [19] for  $e^+e^- \rightarrow WW \rightarrow 4f$  can be taken over to  $\gamma\gamma$  collisions with minor modifications.

The combination of virtual and real-photon corrections is non-trivial for two reasons. First, the finite-fermion-mass effects have to be restored in the phase-space regions of collinear photon radiation off charged fermions, and the IR regularization for soft-photon emission has to be implemented. To this end, we employ the dipole subtraction formalism for photon radiation [20] as well as the more conventional phase-space slicing approach. The second subtlety concerns the fact that we apply the DPA only to the virtual corrections, but not to the real-photon parts. Therefore, the cancellation of soft and collinear singularities has to be done carefully, in order to avoid mismatch.

Finally, the Higgs-boson resonance in the  $s$ -channel has to be treated with care. Firstly, the Higgs decay width has to be introduced in the amplitude without violating gauge invariance. We separate the gauge-invariant resonance pole and include the width only in the resonant part which is proportional to its gauge-invariant residue. Secondly, although the Higgs resonance is loop-induced, it is not sufficient to include the interference between its contribution  $\mathcal{M}_{\text{Higgs}}$  to the amplitude with the Born amplitude, but it is necessary to include the square  $|\mathcal{M}_{\text{Higgs}}|^2$  in the squared amplitude, in order to get a proper description of the resonance.

## 3.2. Numerical results

The cross section for  $\gamma\gamma \rightarrow \nu_e e^+ d\bar{u}$ , including the convolution over the photon spectrum, is shown in Figure 2 as a function of CM energy  $\sqrt{s_{ee}}$  for a Higgs mass of  $M_H = 130 \text{ GeV}$  and in the lower left plot also for  $M_H = 170 \text{ GeV}$ . The remaining input parameters as well as the precise setup of the calculation are given in Ref. [4]. In the upper plots the absolute prediction is shown and in the lower plots the corrections relative to the Born cross section. The interesting structure in the lower left plot reflects the shape of the photon spectrum convoluted with the Higgs resonance. Since

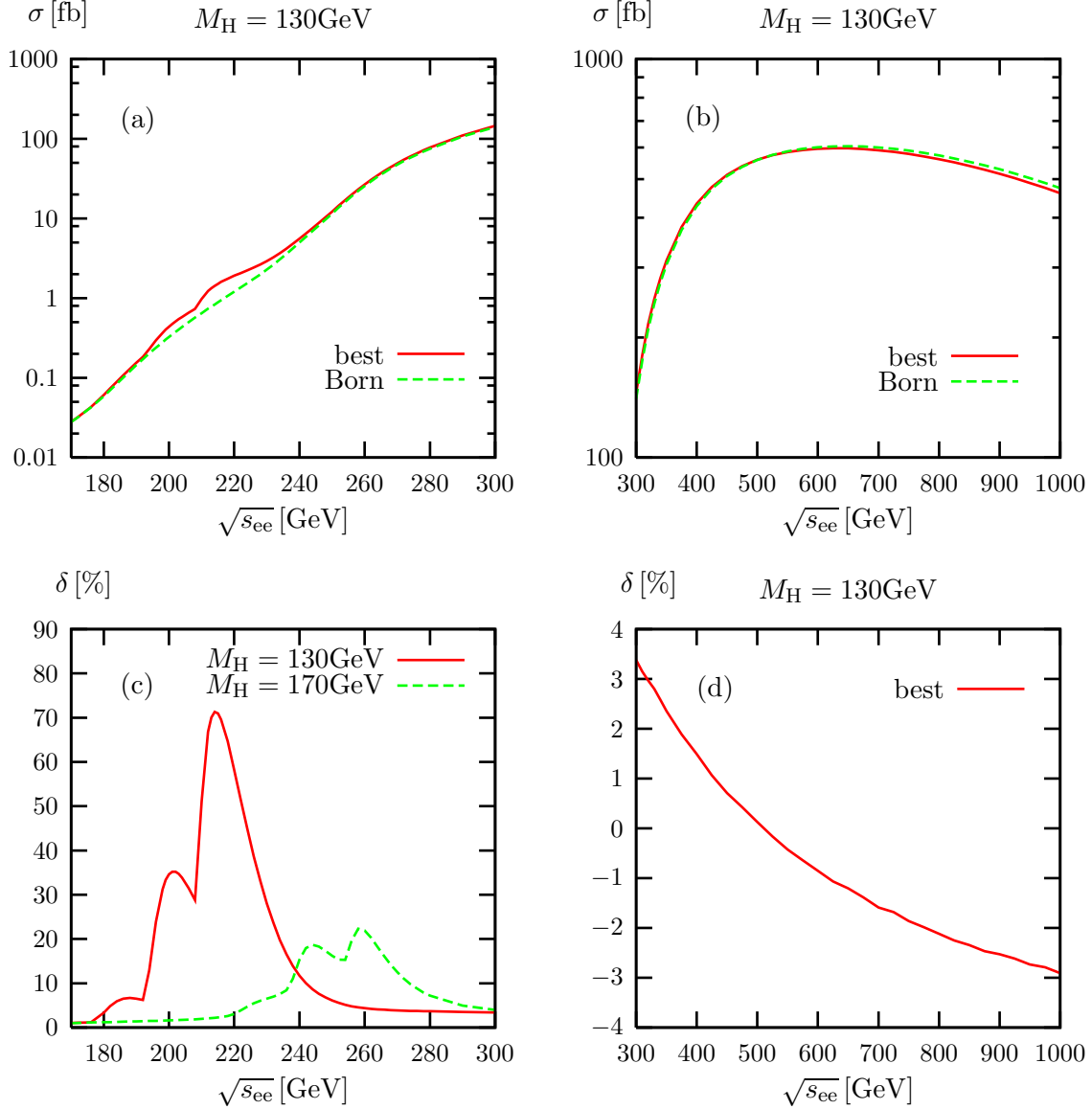


Figure 2: Integrated cross section for  $\gamma\gamma \rightarrow \nu_e e^+ d\bar{u}$  (upper plots) and relative radiative corrections (lower plots) including the convolution over the photon spectrum for  $M_H = 130$  GeV and 170 GeV (l.h.s.). For  $\sqrt{s_{ee}} > 300$  GeV (r.h.s.) the “best” curve for  $M_H = 170$  GeV practically coincides with the shown curve for  $M_H = 130$  GeV. (Taken from Ref. [4].)

the Higgs resonance is very narrow, a sizable contribution is only possible if  $x_1 x_2 s_{ee} \approx M_H^2$  where  $x_1$  and  $x_2$  are the energy fractions carried by the photons. The correction is very small at low  $\sqrt{s_{ee}}$  where  $x_1$  and  $x_2$  both have to be so large in order to match this condition that the corresponding spectrum is extremely small. Increasing  $\sqrt{s_{ee}}$  allows for lower values of  $x_1$  and  $x_2$ . For instance, for  $M_H = 130$  GeV, the rise at  $\sqrt{s_{ee}} \sim 180$  GeV results from a region where both  $x_1$  and  $x_2$  are in the high-energy tail of the spectrum which is produced by multiple photon scattering. The peak at  $\sqrt{s_{ee}} \sim 200$  GeV is caused by events where one photon comes from the high-energy tail and one from the dominant peak in the photon spectrum. Finally, at  $\sqrt{s_{ee}} \gtrsim 210$  GeV both  $x_1$  and  $x_2$  originate from the dominant photon-spectrum peak which causes the steep rise until  $\sqrt{s_{ee}} \sim 220$  GeV. For energies above the Higgs resonance [see Figure 2(d)] the corrections decrease and stay in the range of a few per cent up to TeV energies.

In Figure 3 we show the invariant-mass and production-angle distributions of the  $W^-$  boson as reconstructed from the  $d\bar{u}$  pair in the process  $\gamma\gamma \rightarrow \nu_e e^+ d\bar{u}$ , both with and without convolution over the photon spectrum. The upper

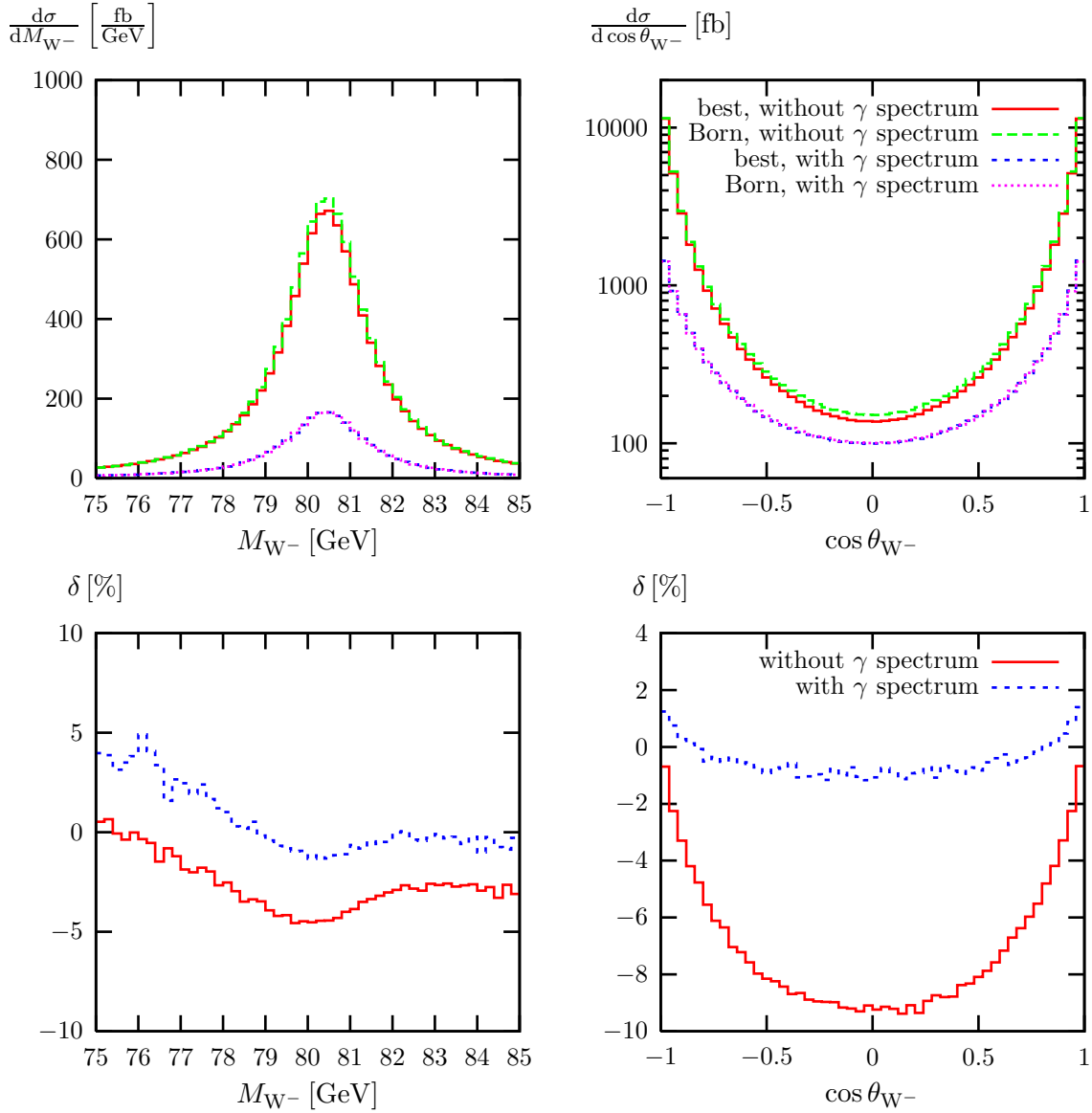


Figure 3: Absolute predictions (upper plots) and relative corrections (lower plots) for the invariant-mass (l.h.s.) and production-angle (r.h.s.) distributions of the  $W^-$  bosons reconstructed from the  $d\bar{u}$  pairs in the process  $\gamma\gamma \rightarrow \nu_e e^+ d\bar{u}$  at  $\sqrt{s} = 500$  GeV (Taken from Ref. [4]).

plots show the absolute predictions and the lower plots the corrections normalized to the Born predictions. Since we use  $\sqrt{s_{\gamma\gamma}} = 500$  GeV and  $\sqrt{s_{ee}} = 500$  GeV, the corrections are shifted upwards when including the photon spectrum, because the effective energy of the photons is lower. For the W-invariant-mass distribution, the shape of the correction, however, is hardly changed by the convolution over the photon spectrum. As the shape of the corrections determines a possible shift of the peak of the invariant-mass distribution, it is of particular importance in the determination of the W-boson mass. The measurement of the W-boson mass can, e.g., be used for understanding and calibrating the detector of a  $\gamma\gamma$  collider. The distribution in the W-boson production angle is sensitive to anomalous couplings. In order to set bounds on these couplings it is mandatory to know radiative corrections, because both anomalous couplings and radiative corrections typically distort angular distributions. While the correction without the photon spectrum is about  $-9\%$  for W bosons emitted perpendicular to the beam, the corrections are rather small when including the photon spectrum. In fact, the relative correction  $\delta$  is accidentally small at  $\sqrt{s_{ee}} \sim 500$  GeV [cf. Figure 2(d)] and might also become larger if other cuts or event selection procedures are applied.

## References

- [1] I. F. Ginzburg *et al.*, Nucl. Instrum. Meth. **205** (1983) 47 and Nucl. Instrum. Meth. A **219** (1984) 5;  
V. I. Telnov, Nucl. Instrum. Meth. A **294** (1990) 72;  
R. Brinkmann *et al.*, Nucl. Instrum. Meth. A **406** (1998) 13 [hep-ex/9707017];  
I. Watanabe *et al.*, “ $\gamma\gamma$  collider as an option of JLC,” KEK-REPORT-97-17;  
B. Badelek *et al.* “TESLA TDR, Part VI, Chapter 1: Photon collider at TESLA,” hep-ex/0108012;  
T. Abe *et al.* [American Linear Collider Working Group Collaboration], SLAC-R-570, *Resource book for Snow-mass 2001* [hep-ex/0106055, hep-ex/0106056, hep-ex/0106057, hep-ex/0106058].
- [2] A. De Roeck, hep-ph/0311138;  
M. Krawczyk, hep-ph/0312341;  
S. J. Brodsky, hep-ph/0404186.
- [3] A. Bredenstein, S. Dittmaier and M. Roth, Eur. Phys. J. C **36** (2004) 341 [hep-ph/0405169].
- [4] A. Bredenstein, S. Dittmaier and M. Roth, hep-ph/0506005.
- [5] M. Moretti, Nucl. Phys. B **484** (1997) 3 [hep-ph/9604303] and hep-ph/9606225;  
M. Baillargeon, G. Bélanger and F. Boudjema, Phys. Lett. B **404** (1997) 124 [hep-ph/9701368] and Nucl. Phys. B **500** (1997) 224 [hep-ph/9701372];  
E. Boos and T. Ohl, Phys. Lett. B **407** (1997) 161 [hep-ph/9705374].
- [6] A. F. Zarnecki, Acta Phys. Polon. B **34** (2003) 2741 [hep-ex/0207021].
- [7] W. Kilian, “WHIZARD 1.0: A generic Monte-Carlo integration and event generation package for multi-particle processes. Manual,” LC-TOOL-2001-039.
- [8] T. Stelzer and W. F. Long, Comput. Phys. Commun. **81** (1994) 357 [hep-ph/9401258].  
H. Murayama, I. Watanabe and K. Hagiwara, “HELAS: HELicity amplitude subroutines for Feynman diagram evaluations,” KEK-91-11.
- [9] M. W. Grünewald *et al.*, in *Reports of the Working Groups on Precision Calculations for LEP2 Physics*, eds. S. Jadach, G. Passarino and R. Pittau (CERN 2000-009, Geneva, 2000), p. 1 [hep-ph/0005309].
- [10] A. Denner, S. Dittmaier, M. Roth and L. H. Wieders, Phys. Lett. B **612** (2005) 223 [hep-ph/0502063] and hep-ph/0505042.
- [11] A. Denner, S. Dittmaier, M. Roth and D. Wackeroth, Nucl. Phys. B **560** (1999) 33 [hep-ph/9904472]; Phys. Lett. B **475** (2000) 127 [hep-ph/9912261]; Eur. Phys. J. direct C **2** (2000) 4 [hep-ph/9912447]; Nucl. Phys. B **587** (2000) 67 [hep-ph/0006307]; hep-ph/0101257 and Comput. Phys. Commun. **153** (2003) 462 [hep-ph/0209330].
- [12] A. Aeppli, G. J. van Oldenborgh and D. Wyler, Nucl. Phys. B **428** (1994) 126 [hep-ph/9312212].
- [13] S. Jadach *et al.*, Phys. Rev. D **61** (2000) 113010 [hep-ph/9907436]; Phys. Rev. D **65** (2002) 093010 [hep-ph/0007012]; Comput. Phys. Commun. **140** (2001) 432 [hep-ph/0103163] and Comput. Phys. Commun. **140** (2001) 475 [hep-ph/0104049].
- [14] W. Beenakker, F. A. Berends and A. P. Chapovsky, Nucl. Phys. B **548** (1999) 3 [hep-ph/9811481].
- [15] Y. Kurihara, M. Kuroda and D. Schildknecht, Phys. Lett. B **509** (2001) 87 [hep-ph/0104201].
- [16] A. Denner, S. Dittmaier and R. Schuster, Phys. Rev. D **51** (1995) 4738 [hep-ph/9411268] and Nucl. Phys. B **452** (1995) 80 [hep-ph/9503442].
- [17] G. Jikia, Nucl. Phys. B **494** (1997) 19 [hep-ph/9612380].
- [18] D. Y. Bardin, S. Riemann and T. Riemann, Z. Phys. C **32** (1986) 121;  
F. Jegerlehner, Z. Phys. C **32** (1986) 425 [Erratum-ibid. C **38** (1988) 519];  
A. Denner and T. Sack, Z. Phys. C **46** (1990) 653.
- [19] K. Melnikov and O. I. Yakovlev, Nucl. Phys. B **471** (1996) 90 [hep-ph/9501358];  
W. Beenakker, A. P. Chapovsky and F. A. Berends, Phys. Lett. B **411** (1997) 203 [hep-ph/9706339] and Nucl. Phys. B **508** (1997) 17 [hep-ph/9707326];  
A. Denner, S. Dittmaier and M. Roth, Nucl. Phys. B **519** (1998) 39 [hep-ph/9710521].
- [20] S. Dittmaier, Nucl. Phys. B **565** (2000) 69 [hep-ph/9904440];  
M. Roth, PhD thesis, ETH Zürich No. 13363 (1999), hep-ph/0008033.